**Proceedings of the 17th World Congress**
**The International Federation of Automatic Control**
**Seoul, Korea, July 6-11, 2008**

# Robust $H^\infty$ control of hysteresis in a piezoelectric stack actuator ⋆

**Ning Chuang*** **Ian R. Petersen****

*,** *School of Information Technology and Electrical Engineering, University of New South Wales at the Australian Defence Force Academy, Canberra ACT 2600, Australia (e-mail: ning.chuang@adfa.edu.au, i.r.petersen@gmail.com)*

**Abstract:** This paper describes a method for controlling a piezoelectric stack actuator with hysteresis nonlinearity. The actuator used is a high-performance monolithic multilayer piezo actuator. The proposed control method involves a circuit, which was built with a capacitor in series with the piezo actuator to provide a measured output voltage which is proportional to the charge on the piezo actuator. The controller is designed based on a model of the hysteresis nonlinearity constructed using experimental data. The paper considers a robust $H^\infty$ tracking controller to control the piezoelectric actuator. The controller is designed using an uncertain system model. Simulation results show that the controller can significantly reduce the effect of the hysteresis nonlinearity.

Keywords: Piezoelectric stack actuators, hysteresis, nonlinear systems, charge-control, $H^\infty$ control, robust control.

## 1. INTRODUCTION

This paper considers the control of a piezoelectric stack actuator (PEA) and shows how the hysteresis nonlinearity can be controlled using robust $H^\infty$ control. The piezoelectric stack actuator used was a P-882.51 manufactured by PI in Germany. Piezoelectric stack actuators have important applications to Atomic Force Microscopes and Nano-positioning systems; e.g., see Croft et al. (2000), Leang and Devasia (2006), Goldfarb and Celanovic (1997), and Sebastian and Salapaka (2005). A number of previous papers have considered the modeling of piezoactuators to account for properties such as creep and hysteresis; e.g., see Ru and Sun (2005), Jung et al. (2001), and Banning et al. (2001). In the paper (Croft et al. (2000)), the application of piezoelectric actuators to scanning probe microscopy was considered, and a model-based inversion control technique was developed. This paper showed that substantial improvements in positioning precision and operating speed could be obtained. However the method relied on having an accurate model of the nonlinearity.

With the rapid development of nano-positioning and AFM applications for piezoelectric actuators, the control of such actuators has become an important topic. A significant challenge in the use of piezoelectric actuators in such an application is the existence of hysteresis which limits the accuracy of position control. This motivates us to utilize robust $H^\infty$ control theory, to control piezoelectric actuator systems with hysteresis nonlinearity.

Our approach to the control of hysteresis in a piezoelectric actuator is adapted from the charge control method, such as can be found in Salah et al. (2007) and Moheimani and Vautier (2005). In these papers, it was noted that the use of charge control could lead to reduced hysteresis in a piezoelectric stack actuator. One difference between our approach and the approach of Adriaens et al. (2000) is that no mechanical measurement was used in our piezoelectric actuator control system. Our control system was configured by connecting an external capacitor in series with the piezo actuator and measuring the voltage across this capacitor which is proportional to the charge in the piezoelectric stack actuator; see also Salah et al. (2007).

The method we used for modeling the piezoelectric actuator is derived from the approach of the paper Adriaens et al. (2000), in which a nonlinear model of the hysteresis voltage versus the charge was proposed. There was very good agreement between our model and experimental test data which was obtained using a dSpace DSP system. We also designed a robust $H^\infty$ controller to control the effect of hysteresis in this stack actuator. The method used for designing our controller was obtained from the approach of Xie et al. (1992) and Xie and de Souza (1992). In order to apply this approach we treat the hysteresis as a sector bounded uncertainty. These results enabled the robust $H^\infty$ control problem to be converted into a standard $H^\infty$ control problem which could be solved using Riccati equation methods; e.g., see Petersen et al. (1991). The closed loop system corresponding to our robust $H^\infty$ controller was analyzed via Simulink simulations. These simulations verified that our robust $H^\infty$ controller can significantly reduce the effect of hysteresis in the piezoelectric actuator.

## 2. MODELING THE PIEZOELECTRIC ACTUATOR

Our model for the piezoelectric stack actuator is based on the approach of Adriaens et al. (2000), which uses a description consisting of electrical and mechanical elements. In Adriaens et al. (2000), the PEA system is modeled using the electromechanical model shown in Figure 1.

⋆ This work was supported by the Australian Research Council.

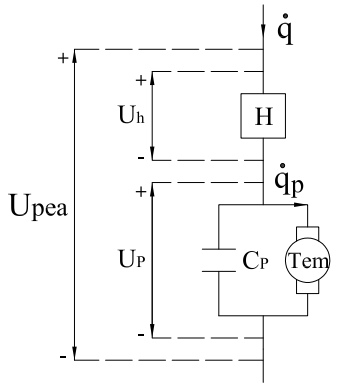


Fig. 1. Electromechanical model of the PEA.

An expression for the interaction force $F_P$ in this model is:

$$F_P = T_{em} U_P = m\ddot{y} + c\dot{y} + k\,y \tag{1}$$

In equation (1), $y$ represents the mechanical displacement and the interaction force depends on the mechanical parameters of mass $m$, damping coefficient $c$ and stiffness $k$. Also, $T_{em}$ is defined as the transformer ratio for the electromechanical transducer. Using the electromechanical model in Figure 1, we can obtain an equivalent circuit of our complete piezo system as shown in Figure 2.

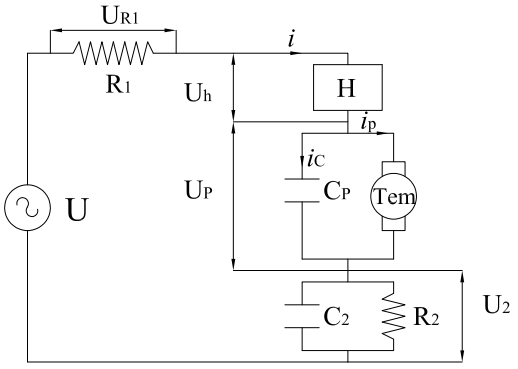


Fig. 2. Piezoelectric stack actuator model.

Here $U$ represents the amplifier voltage applied to the circuit, $R_1$ represents the Thevenin equivalent resistance of the power amplifier, $C_2$ is the external capacitor in series with the piezoelectric stack actuator, $U_2$ is the capacitor voltage measured using a differential probe, $R_2$ is the resistance of the differential probe. Using a standard analogy between electrical and mechanical systems applied to (1) we can replace the mechanical elements by an equivalent electric circuit as shown in Figure 3.

Here $R$, $L$ and $C$ can be calculated from the mechanical parameters as $R = \frac{c}{Tem^2}$, $L = \frac{m}{Tem^2}$ and $C = \frac{k}{Tem^2}$. In Adriaens et al. (2000), the hysteresis nonlinearity between the hysteresis voltage $U_h$ and the charge $q$ in the model is described by the equation:

$$\dot{q} = \alpha|\dot{U}_h|(a\,U_h - q) + b\,\dot{U}_h \tag{2}$$

where $\alpha$, $a$ and $b$ are constants which determine the shape of the nonlinearity. From this, it can be seen that the size of the hysteresis nonlinearity in the piezoelectric actuator

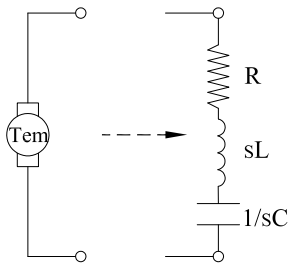


Fig. 3. Equivalent RLC circuit.

depends on the value of $\alpha$. If $\alpha$ is small enough, we can consider the system as a linear system. Using (2), a nonlinear relationship between the current $i$ in the piezo and the voltage generated by the hysteresis $U_h$ can be derived as follows:

$$\dot{q} = i = \begin{cases} (b + \alpha(a\,U_h - q))\,\dot{U}_h & \text{if } \dot{U}_h \geq 0; \\ (b - \alpha(a\,U_h - q))\,\dot{U}_h & \text{if } \dot{U}_h < 0. \end{cases} \tag{3}$$

Hence, the model in Figure 2 can be replaced by an equivalent electrical circuit, as shown in Figure 4.

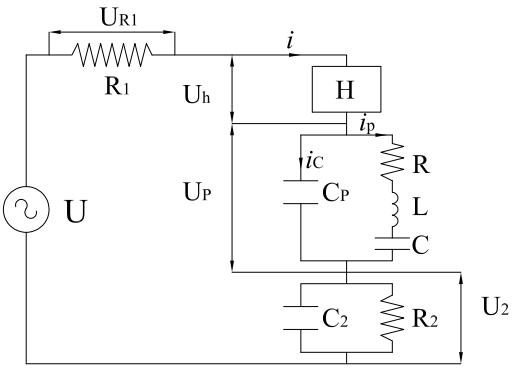


Fig. 4. Piezoelectric actuator equivalent circuit.

The state variables for the equivalent electrical circuit model in Figure 4 are defined as $x_1 = i_P$, $x_2 = U_C$, $x_3 = U_2$, $x_4 = U_h$ and $x_5 = q$. This leads to a state space model for the piezo actuator circuit as follows:

$$\begin{aligned}
\dot{x}_1 &= \dot{i}_P = -\frac{R}{L\,C_P}x_1 - \frac{C + C_P}{L\,C_P}x_2 + \frac{1}{L\,C_P}x_5; \\
\dot{x}_2 &= \dot{U}_C = \frac{1}{C}i_P = \frac{1}{C}x_1; \\
\dot{x}_3 &= \dot{U}_2 = \frac{C}{R_1\,C_2\,C_P}x_2 - \left(\frac{1}{R_1\,C_2} + \frac{1}{R_2\,C_2}\right)x_3 \\
&\quad - \frac{1}{R_1\,C_2}x_4 - \frac{1}{R_1\,C_2\,C_P}x_5 + \frac{1}{R_1\,C_2}U; \\
\dot{x}_4 &= \dot{U}_h = \begin{cases} \dfrac{\frac{C}{C_P}x_2 - x_3 - x_4 - \frac{1}{C_P}x_5 + U}{R_1(b + \alpha(ax_4 - x_5))} & \text{if } i \geq 0; \\ \dfrac{\frac{C}{C_P}x_2 - x_3 - x_4 - \frac{1}{C_P}x_5 + U}{R_1(b - \alpha(ax_4 - x_5))} & \text{if } i < 0; \end{cases} \\
\dot{x}_5 &= \dot{q} = \frac{C}{R_1 C_P}x_2 - \frac{1}{R_1}x_3 - \frac{1}{R_1}x_4 - \frac{1}{R_1 C_P}x_5 + \frac{1}{R_1}u.
\end{aligned} \tag{4}$$

where $i = \dot{q}$ as in (3).

In our experimental set up, the actuator was unloaded and the unloaded resonate frequency of the actuator is approximately 70 $kHz$ which is well beyond the frequency range of interest. This means that we can obtain a simplified nonlinear model for the system by setting $T_{em}$ to zero. This implies that the electromechanical elements need no longer be included in the model. Then, a simplified equivalent circuit can be obtained as shown in Figure 5.

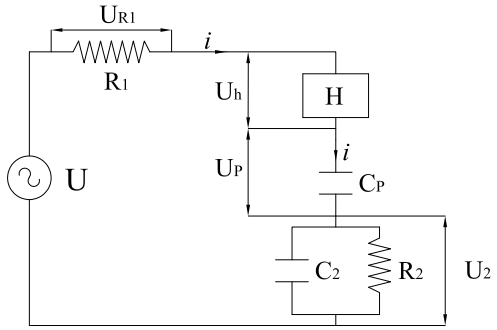


Fig. 5. Simplified equivalent circuit model.

In this case, only three state variables, $x_1 = U_2$, $x_2 = U_h$ and $x_3 = q$ are needed. Then, we can write the corresponding state space equations as follows:

$$\begin{aligned}
\dot{x}_1 = \dot{U}_2 &= -(\frac{1}{R_1C_2} + \frac{1}{R_2C_2})x_1 - \frac{1}{R_1C_2}x_2 \\
&\quad -\frac{1}{R_1C_2C_P}x_3 + \frac{1}{R_1C_2}U; \\
\dot{x}_2 = \dot{U}_h &= \begin{cases} \dfrac{-x_1 - x_2 - \frac{1}{C_P}x_3 + U}{R_1(b + \alpha(ax_2 - x_3))} & \text{if } i \geq 0; \\ \dfrac{-x_1 - x_2 - \frac{1}{C_P}x_3 + U}{R_1(b - \alpha(ax_2 - x_3))} & \text{if } i < 0; \end{cases} \\
\dot{x}_3 &= \dot{q} = -\frac{1}{R_1}x_1 - \frac{1}{R_1}x_2 - \frac{1}{R_1C_P}x_3 + \frac{1}{R_1}u. \qquad (5)
\end{aligned}$$

and, $\dot{q} = i$ as previously defined.

## 3. NONLINEAR MODEL PERFORMANCE

### *3.1 System identification and model realization*

In the piezoelectric actuator equivalent circuit of Figure 5, the output of the system was specified as $U_2$ which was measured experimentally. The state equations for a corresponding linear model are obtained by setting $\alpha = 0$ in (5) which leads to the following linear state space model:

$$\begin{aligned}
\dot{x} &= \begin{bmatrix} -(\frac{1}{R_1C_2} + \frac{1}{R_2C_2}) & -\frac{1}{R_1C_2} & -\frac{1}{R_1C_2C_P} \\ -\frac{1}{R_1b} & -\frac{1}{R_1b} & -\frac{1}{R_1bC_P} \\ -\frac{1}{R_1} & -\frac{1}{R_1} & -\frac{1}{R_1C_P} \end{bmatrix} x \\
&\quad + \begin{bmatrix} \frac{1}{R_1C_2} \\ \frac{1}{R_1b} \\ \frac{1}{R_1} \end{bmatrix} u; \\
&= Ax + Bu. \qquad (6)
\end{aligned}$$

The system output $y = U_2$ in this linear model is determined by the equation $y = Cx$ where $C = [\ 1\ 0\ 0\ ]$. The parameters in this model were measured directly as follows:

$$\begin{aligned}
b &= 9 \times 10^{-7}F; \\
R_1 &= 4.85\Omega; \\
R_2 &= 8 \times 10^{6}\Omega; \\
C_P &= 6 \times 10^{-7}F; \\
C_2 &= 9.91 \times 10^{-8}F.
\end{aligned}$$

The static capacitance of the piezoelectric stack actuator was measured at $360nF$ which is the value of $b$ in series with $C_P$.

### *3.2 Hysteresis model and experimental test results*

The nonlinear state space model (5) was implemented in Simulink. Also, the nonlinearity parameters were chosen as $a = 9 \times 10^{-9}$ and $\alpha = 0.048$ so that the simulation results matched the experimental test data. The piezoelectric actuator was tested using a dSpace DSP system, as shown in Figure 6.

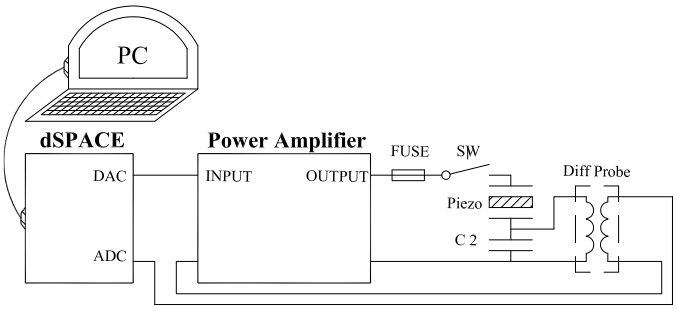


Fig. 6. dSPACE experimental test setup.

We plotted the experimental test results obtained from the piezo stack actuator together with a simulated hysteresis curve. A comparison of the two hysteresis curves for the model and the experimental data is illustrated in Figure 7. In this plot, the experimental value of the charge $q$ was calculated from the output voltage $U_2$ as $q = C_2\,U_2$.

## 4. DESIGN OF A ROBUST $H^\infty$ CONTROLLER

A robust $H^\infty$ control method was employed to design a tracking controller, in which the charge tracked a reference input. As in Moheimani and Vautier (2005), it was expected that this charge control method could reduce the effect of hysteresis. Once we had constructed

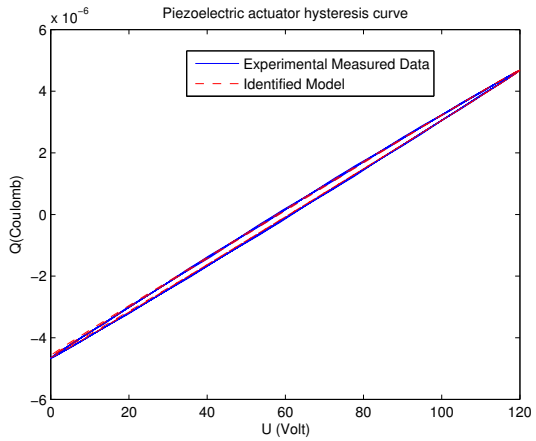


Fig. 7. $Q$ versus $U$ obtained from experimental test data and model simulations.

a hysteresis model for the piezo stack actuator circuit, we then considered a design of a robust $H^\infty$ controller with norm-bounded time-varying uncertainty via output feedback using the approach of Xie et al. (1992) and Xie and de Souza (1992). Using equation (3), we can see that the hysteresis nonlinearity can be regarded as a sector bounded nonlinearity, provided we have an upper bound on the magnitude of the quantity $\alpha U_h - q$. This is illustrated in Figure 8.

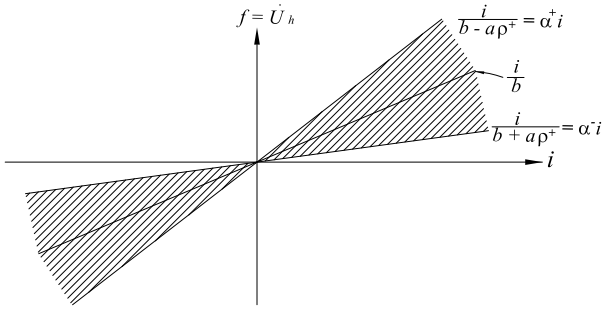


Fig. 8. Sector bounded nonlinearity in the piezo stack actuator model.

Here, we can write $\rho = a\,U_h - q$, and $\dot{U}_h = f(i,\rho) = \frac{i}{b \pm \alpha\,|\rho|}$. Then, we can define the sector bounded between the lines $f = \alpha^+ i$ and $f = \alpha^- i$, in which $\alpha^+ > \alpha^- > 0$, and $\alpha^+ = \frac{i}{b - \alpha\,\rho^+}$ and $\alpha^- = \frac{i}{b + \alpha\,\rho^+}$. Here $\rho^+$ is the maximum expected value of the quantity $|\rho|$. Using our nonlinear model, the value of $\rho^+ = 4.65 \times 10^{-6}$ was obtained from a simulation of the PEA with a 120 Volt peak-peak sinusoidal voltage applied. According to the manufacturer's specifications, this is the maximum voltage which can be applied to the PEA.

Also, we let

$$\alpha_o = \frac{\alpha^+ + \alpha^-}{2} \qquad \text{and} \qquad \Delta_\alpha = \frac{\alpha^+ - \alpha^-}{2}.$$

This gives

$$\begin{aligned} \alpha^+ &= \alpha_o + \Delta_\alpha; \\ \alpha^- &= \alpha_o - \Delta_\alpha. \end{aligned}$$

where $\alpha_o = \frac{b}{b^2 - \alpha^2\,\rho^{+2}}$ and $\Delta_\alpha = \frac{\alpha\,\rho}{b^2 - \alpha^2\,\rho^{+2}}$. Also note that the equation for $i$ in (5) can be expressed as $i = E_1 x + E_2 u$, which can be adapted into the uncertainty description considered in Xie and de Souza (1992) as follows:

$$\begin{aligned} [\,\Delta A\ \Delta B\,] \begin{bmatrix} x \\ u \end{bmatrix} &= H_1\,\Delta\,[E_1 x + E_2 u] \\ &= H_1\,\xi. \end{aligned} \tag{7}$$

where

$$\xi = \Delta\,\zeta,\ \zeta = E_1 x + E_2 u,\ \|\Delta\| \le 1 \text{ and } H_1 = [\,0\ \Delta_\alpha\ 0\,]^T.$$

This leads to the uncertain system model:

$$\begin{aligned} \dot{x} &= A\,x + H_1\,\xi + B_2\,u; \\ \zeta &= E_1 x + E_2 u; \\ y &= C\,x. \end{aligned} \tag{8}$$

Also for our uncertain system model, the state equations for the linear part of the model are given as:

$$\begin{aligned} \dot{x} &= Ax + [\,H_1\ B_2\,] \begin{bmatrix} \xi \\ u \end{bmatrix}; \\ \begin{bmatrix} \zeta \\ y \end{bmatrix} &= \begin{bmatrix} E_1 \\ C \end{bmatrix} x + \begin{bmatrix} 0 & E_2 \\ 0 & 0 \end{bmatrix} \begin{bmatrix} \xi \\ u \end{bmatrix}. \end{aligned} \tag{9}$$

It should be noted that for the piezo system under consideration, the state space model (9) is not minimal. Hence, we can replace these state equations with a corresponding minimal realization as in equation (10):

$$\begin{aligned} \dot{x}_r &= A_r x_r + [\,H_{1r}\ B_{2r}\,] \begin{bmatrix} \xi \\ u \end{bmatrix}; \\ \begin{bmatrix} \zeta \\ y \end{bmatrix} &= \begin{bmatrix} E_{1r} \\ C_r \end{bmatrix} x_r + \begin{bmatrix} 0 & E_{2r} \\ 0 & 0 \end{bmatrix} \begin{bmatrix} \xi \\ u \end{bmatrix}. \end{aligned} \tag{10}$$

A robust $H^\infty$ tracking control problem is then set up as shown in Figure 9. In this problem, $w$ is the reference input and $z$ is the error output. The filter has been introduced because the plant output cannot be expected to track the reference input at very low frequencies or very high frequencies.

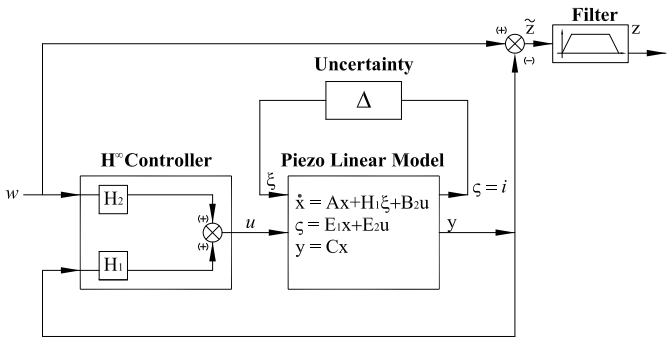


Fig. 9. Structure of the robust $H^\infty$ tracking control problem under consideration.

Accordingly, a state space model corresponding to this problem including the filter can be written as follows:

$$\dot{\widetilde{x}} = \begin{bmatrix} \dot{x_r} \\ \dot{\eta} \end{bmatrix} = \underbrace{\begin{bmatrix} A_r & 0 \\ -B_f C_r & A_f \end{bmatrix}}_{\widetilde{A}} \begin{bmatrix} x_r \\ \eta \end{bmatrix} + \underbrace{\begin{bmatrix} 0 & 0 \\ B_f & 0 \end{bmatrix}}_{\widetilde{B}_1} \begin{bmatrix} w \\ \widetilde{w} \end{bmatrix} + \underbrace{\begin{bmatrix} B_{2r} \\ 0 \end{bmatrix}}_{\widetilde{B}_2} u + \underbrace{\begin{bmatrix} H_{1r} \\ 0 \end{bmatrix}}_{\widetilde{H}_1} \xi;$$
$$= \widetilde{A}\widetilde{x} + \widetilde{B}_1 w + \widetilde{B}_2 u + \widetilde{H}_1 \xi. \quad (11)$$

Here $\eta$ is the state of the filter system:

$$\dot{\eta} = A_f \eta + B_f \widetilde{z};$$
$$z = C_f \eta. \quad (12)$$

The filter was chosen to have a transfer function:

$$G(s) = \frac{1000(s+\epsilon_1)}{(s+1)(s+1000)}$$

where $\epsilon_1$ is treated as a design parameter.

The outputs $z$ and $\widetilde{y}$ of the overall system in Figure 9 can be obtained from the following equations:

$$z = \underbrace{[\,0 \;\; C_f\,]}_{\widetilde{C}_1} \begin{bmatrix} x_r \\ \eta \end{bmatrix} + \underbrace{\begin{bmatrix} 0 \\ 0 \end{bmatrix}}_{\widetilde{D}_{12}} u;$$
$$\widetilde{y} = \begin{bmatrix} y \\ w \end{bmatrix} = \underbrace{\begin{bmatrix} C_r & 0 \\ 0 & 0 \end{bmatrix}}_{\widetilde{C}_2} \begin{bmatrix} x_r \\ \eta \end{bmatrix} + \underbrace{\begin{bmatrix} 0 & \epsilon_2 \\ 1 & 0 \end{bmatrix}}_{\widetilde{D}_{21}} \begin{bmatrix} w \\ \widetilde{w} \end{bmatrix}. \quad (13)$$

Note that, in order to satisfy the standard $H^\infty$ conditions, we have introduced a new disturbance input $\widetilde{w}$ which acts as a measurement disturbance added to the measured reference signal $w$. This disturbance is scaled by $\epsilon_2$ which is treated as a design parameter.

In our case, Equation (7) needs to be modified to correspond to the uncertainty in the overall system as follows:

$$[\,\Delta\widetilde{A} \;\; \Delta\widetilde{B}\,] = \widetilde{H}_1 \Delta [\,\widetilde{E}_1 \;\; \widetilde{E}_2\,]. \quad (14)$$

Hence, the uncertainty output signal $\zeta$ (i.e., the current $i$) can be rewritten in terms of the complete state space model as:

$$\zeta = \underbrace{[\,E_1 \;\; 0\,]}_{\widetilde{E}_1} \begin{bmatrix} x \\ \eta \end{bmatrix} + \underbrace{[\,E_2\,]}_{\widetilde{E}_2} u. \quad (15)$$

We now construct the robust $H^\infty$ controller by applying the results of Xie et al. (1992) to the uncertain system defined by the equations (11), (13), (15). This leads us to consider a standard $H^\infty$ problem defined by the following state equations:

$$\dot{x} = \widetilde{A}x + [\,\sqrt{\epsilon}\,\varrho\,\widetilde{H}_1 \;\; \gamma^{-1}\widetilde{B}_1\,]\,\widetilde{w} + \widetilde{B}_2 u;$$
$$\widetilde{z} = \begin{bmatrix} \frac{1}{\sqrt{\epsilon}}\widetilde{E}_1 \\ \widetilde{C}_1 \end{bmatrix} x + \begin{bmatrix} \frac{1}{\sqrt{\epsilon}}\widetilde{E}_2 \\ \widetilde{D}_{12} \end{bmatrix} u; \quad (16)$$
$$y = \widetilde{C}_2 x + [\,\sqrt{\epsilon}\,\varrho\,\widetilde{H}_2 \;\; \gamma^{-1}\widetilde{D}_{21}\,]\,\widetilde{w}.$$

Here $\epsilon$ is an additional design parameter and $\gamma$ is the desired level of disturbance attenuation. This standard $H^\infty$ problem is then solved via an algebraic Riccati equation approach; e.g., see Petersen et al. (1991). The design parameters used in our case were chosen as follows:

$$\epsilon = 0.1000556;$$
$$\epsilon_1 = 1 \times 10^{-10};$$
$$\epsilon_2 = 9 \times 10^{-7};$$
$$\gamma = 0.1.$$

The controller obtained from this method is applied to the piezoelectric stack actuator as in the block diagram shown in Figure 10.

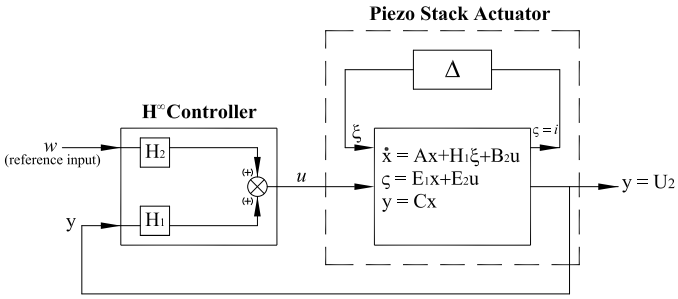


Fig. 10. Block diagram of piezoelectric stack actuator with the $H^\infty$ tracking controller.

Bode plots of the closed loop system are shown in Figure 11, in which the uncertainty $\Delta$ was set at the values of 0 and $\pm 1$ respectively. These Bode plots show that over the frequency range of interest, the transfer function from the reference input to the output is very close to unity.

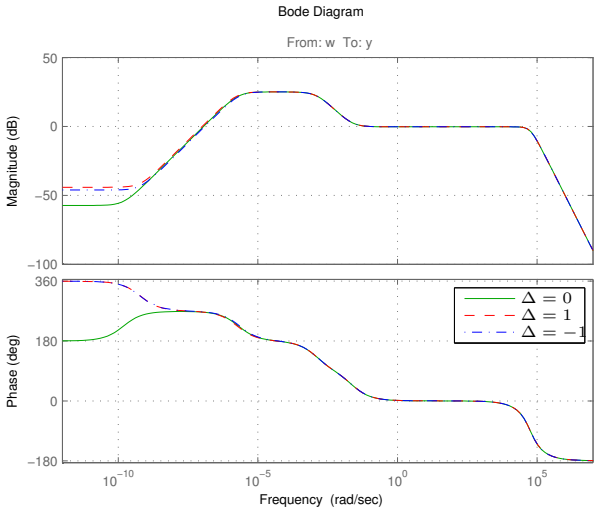


Fig. 11. Closed-loop Bode plots.

An investigation of the performance of the $H^\infty$ controller was carried out in using Simulink and the nonlinear model of the piezoelectric stack actuator (5). We examined the simulation model outputs both using the controller and without using the controller. The results are shown in Figure 12. In this figure, it can be clearly seen that the use of the robust $H^\infty$ controller has significantly reduced the effect of hysteresis.

In addition, we also examined the performance of the controller, in which the reference signal was a sawtooth

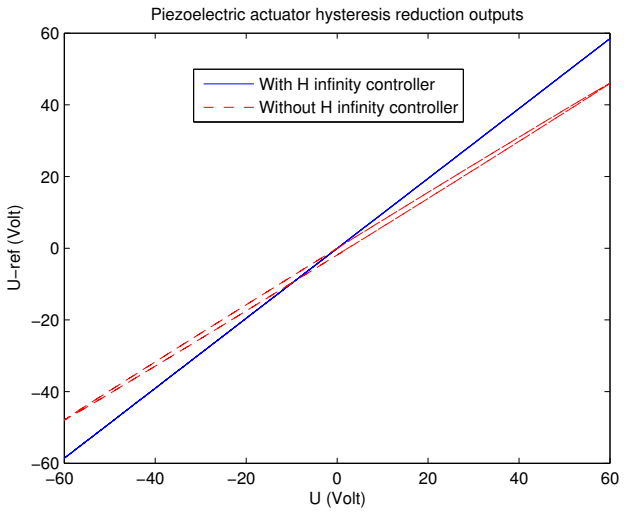


Fig. 12. Hysteresis plot with and without the robust $H^\infty$ controller.

waveform. It should be noted that the manufacturer's specifications for the actuator requires that the applied voltage be in the range of $-20$ to $+120$ volts. Hence, a simulation was carried out using a $0-120$ volt, $5Hz$ sawtooth reference input. The results of this simulation are shown in Figure 13. These simulations show that the output of the system tracks the reference input very closely.

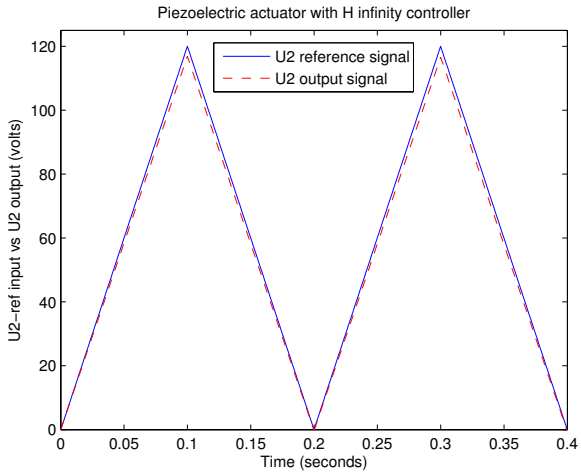


Fig. 13. Controlled piezoelectric actuator with a sawtooth reference input.

## 5. CONCLUSION

The control of hysteresis in a piezoelectric actuator was achieved by using a robust $H^\infty$ control method. Simulation results have demonstrated that hysteresis in a piezoelectric actuator can be significantly reduced using this controller. Simulations were carried out using a model which has shown a good agreement with the experimentally measured hysteresis on the piezoelectric actuator. Future research will be directed towards experimental verification of the simulation results presented in this paper.

## REFERENCES

C. Ru, and L. Sun, Hysteresis and creep compensation for piezoelectric actuator in open-loop operation. *Sensors and Actuators*, Vol.122(A), pp. 124-130, 2005.

H. Jung, J. Y. Shim and D. Gweon, Tracking control of piezoelectric actuators. *Nanotechnology*, Vol.12(1), pp. 14-20, 2001.

R. Banning, W. de Koning, H. Adriaens and R. Koops, State-space analysis and identification for a class of hysteretic systems. *Automatica*, Vol.37(12), pp. 1883-1892, 2001.

D. Croft, G. Shedd and S. Devasia, Creep, Hysteresis, and Vibration Compensation for Piezoactuators: Atomic Force Microscopy Application. *Proceedings of the American Control Conference*, Chicago, Illinons, pp. 2123-2128, Jun. 2000.

K. K. Leang and S. Devasia, Design of hysteresis-compensating iterative learning control for piezo-positioners: Application to atomic force microscopes. *Mechatronics*, Vol.16(3-4), pp. 141-158, 2006.

M. Goldfarb and N. Celanovic, Modeling piezoelectric stack actuators for control of micromanipulation. *IEEE Control Systems Magazine*, Vol.17(3), pp. 69-79, 1997.

A. Sebastian and S. M. Salapaka, Design methodologies for robust nano-positioning. *IEEE Transactions on Control Systems Technology*, Vol.13(6), pp. 868-876, 2005.

M. Salah, M. McIntyre, D. Dawson and J. Wagner, Robust Tracking Control for a Piezoelectric Actuator. *Proceedings of the American Control Conference*, New York, USA, pp. 106-111, Jul. 2007.

S. O. R. Moheimani and B. J. G. Vautier, Resonant control of structural vibration using charge-driven piezoelectric actuators. *IEEE Transactions on Control Systems Technology*, Vol.13(6), pp. 1021-1035, 2005.

H. Adriaens, W. de Koning and R. Banning, Modeling piezoelectric actuators. *IEEE/ASME Transactions on Mechatronics*, Vol.5(4), pp. 331-341, 2000.

L. Xie, M. Fu, and C. E. de Souza, Robust $H_\infty$ Control and Quadratic Stabilization of Systems with Parameter Uncertainty Via Output Feedback. *IEEE Transactions on Automatic Control*, Vol.37(8), pp. 1253-1256, 1992.

L. Xie and C. E. de Souza, Robust $H_\infty$ Control for Linear Systems with Norm-bounded Time-Varying Uncertainty. *IEEE Transactions on Automatic Control*, Vol.37(8), pp. 1188-1191, 1992.

I. R. Petersen, B. D. O. Anderson and E. A. Jonckeere, A first principles solution to the non-singular $H^\infty$ control problem. *International Journal of Robust and Nonlinear Control*, Vol.1(3), pp. 171-185, 1991.